FIZIKA 9 (1977) Supplement 3, 115–140
(Proceedings of the Int. Symp. on Nuclear Collisions and
Their Microscopic Description, Bled, September 1977)

PAULI PRINCIPLE AND ABSORPTION IN HEAVY ION REACTIONS

A. Weiguny

Institut für Theoretische Physik
Universität Münster
West-Deutschland

I. Introduction.

The Pauli principle plays an important role in heavy ion reactions and explains a number of puzzling features of phenomenological approaches: i) Consider the real part U of the optical potential for elastic scattering. Reasonable fits to the experimental data have been obtained by both repulsive core and deep attractive potentials (Fig. 1). At first glance it seems unintelligible that such different types of potentials can be phase-equivalent. We shall see below that the Pauli principle offers an explanation for this type of ambiguity. One would then expect this ambiguity to disappear at high energies where the Pauli principle looses its influence. In fact, with increasing energy the repulsive core is reduced[1] while purely attractive potentials become more and more shallow[2]. Thus the two types of potentials tend to converge to a unique high energy limit. ii) It is often quite difficult to distinguish between refractive and diffractive

effects[3]. For example (Fig. 2) , the typical behaviour of angular distributions at forward angles can often be reproduced by both strong absorptive and refractive models. A rise of the cross section at backward angles is generally assigned to particle exchange which can be described by a real non-local potential. On the other hand, when absorption sets in abruptly as soon as the ions touch, one will obtain reflection[4]. A well-known example is the reflection of electromagnetic waves on a metallic ball. iii) Alpha reduced widths as calculated from the traditional shell model approach are much too small when compared to experiment. The absolute values may be wrong by factors 10 to 1000, varying from light to heavy nuclei. Alpha-cluster models were invoked to remedy the situation but led to unreasonably large alpha-clustering in the nuclear surface, especially for heavy nuclei. Recently, Fliessbach[5] has shown how to remove this discrepancy by proper treatment of antisymmetrization. A similar situation occurs for alpha- and two-nucleon-transfer where the absolute values of spectroscopic factors cannot be explained. In contrast there seems to be no problem in the case of one-nucleon-transfer.

The above examples show the need to develop practicable theories which incorporate Pauli principle and absorption on a fundamental level in a consistent way. Such theories are the resonating group method[6] and the generator coordinate method[7] combined with Feshbach's formalism of effective forces[8].

II. General Framework

a) The Generator Coordinate Method (GCM).

In the GCM the many-body wave function Ψ for elastic scattering is described as superposition of generating functions $\phi(\underset{\sim}{x},\underset{\sim}{r})$,

$$\Psi(\underset{\sim}{x}) = \int \phi(\underset{\sim}{x},\underset{\sim}{r}) f(\underset{\sim}{r}) d\underset{\sim}{r} \quad , \tag{II.1}$$

where x stands for all single-particle coordinates of the nucleons and the parameter $\underset{\sim}{r}$ measures the mean distance between the fragments A and B. The generating functions $\phi(\underset{\sim}{x},\underset{\sim}{r})$ are square-integrable and antisymmetrized with respect to all nucleons of the system; they may be viewed as "snapshots" of the scattering process with the fragments at mean distance $\underset{\sim}{r}$. There are no superfluous degrees of freedom in the theory as the integration in (II.1) extends over all $\underset{\sim}{r}$-values.

The expansion coefficients $f(\underset{\sim}{r})$ are determined by solving the Schrödinger equation of the many-body system in the subspace of Hilbert space spanned by the ansatz (II.1). The result is an infinite set of integral equations ("Griffin-Hill-Wheeler equations"),

$$\int \{H(\underset{\sim}{r}',\underset{\sim}{r}) - EN(\underset{\sim}{r}',\underset{\sim}{r})\} f(\underset{\sim}{r}) d\underset{\sim}{r} = 0 \qquad \text{for all } \underset{\sim}{r}' \quad , \tag{II.2}$$

to be solved with scattering boundary conditions[9] for $f(\underset{\sim}{r})$. In practice, $\phi(\underset{\sim}{x},\underset{\sim}{r})$ will be represented by one or a few Slater determinants in a two-center shell model so that the GCM-kernels

(II.3) $$\left\{ \begin{matrix} H(\underset{\sim}{r}',\underset{\sim}{r}) \\ N(\underset{\sim}{r}',\underset{\sim}{r}) \end{matrix} \right\} = \langle \phi(\underset{\sim}{r}') | \left\{ \begin{matrix} H_{eff} \\ 1 \end{matrix} \right\} | \phi(\underset{\sim}{r}) \rangle$$

can be calculated by standard shell model techniques. H_{eff} is the effective microscopic Hamiltonian in the elastic channel, to be discussed in section IV.

To relate the expansion coefficients $f(\underset{\sim}{r})$ to the wave function of relative motion of fragments A and B, we switch to the

b) Resonating Group Method

where the ansatz (II.1) is replaced by

(II.4) $$\Psi = \phi_{CM} \mathcal{A} \{\phi_A \phi_B g\} \quad .$$

Here ϕ_A and ϕ_B describe the (undistorted) internal structures of A and B, ϕ_{CM} the center-of-mass motion. $\mathcal{A}$ denotes the rest-antisymmetrizer between A and B, and g is the relative motion wave function to be determined.

To this end we project the many-body Schrödinger equation onto the subspace spanned by (II.4),

(II.5) $$(\phi_A \phi_B | H_{err} - E | \Psi) = 0 \quad ,$$

where the round brackets indicate integration over internal fragment coordinates only. The explicit form of the Schrödinger equation of relative motion is obtained by splitting H_{eff} into

(II.6) $$H_{eff} = T_{\underset{\sim}{\rho}} - T_{CM} + H_A + H_B + V_{AB} \quad ,$$

where $\underset{\sim}{\rho}$ is the actual variable of relative motion, and by separating direct and exchange contributions according to

$$\mathcal{A} = 1 + (\mathcal{A} - 1) \quad . \tag{II.6'}$$

The resulting "resonating group equation" reads as follows

$$\{T_{\underset{\sim}{\rho}} + V(\underset{\sim}{\rho}) - \mathcal{E}\}g(\underset{\sim}{\rho}) = \int K(\underset{\sim}{\rho},\underset{\sim}{\rho}')g(\underset{\sim}{\rho}')d\underset{\sim}{\rho}' \quad , \tag{II.7}$$

where

$$V(\underset{\sim}{\rho}) = (\phi_A\phi_B|V_{AB}|\phi_A\phi_B) \tag{II.8}$$

is the direct part of the nucleus-nucleus potential. V is local if the underlying nucleon-nucleon interaction is local, as is assumed in eq. (II.8). The energy $\mathcal{E}$ of relative motion appears after subtracting the internal energies of A and B and the center-of-mass energy from the total energy E. The right hand side in (II.7) contains all exchange contributions (including those of overlap and kinetic energy),

$$-\int K(\underset{\sim}{\rho},\underset{\sim}{\rho}')g(\underset{\sim}{\rho}')d\underset{\sim}{\rho}' = (\phi_A\phi_B|(H_{eff} - E)(\mathcal{A} - 1)|\phi_A\phi_B g) \quad , \tag{II.9}$$

and is non-local like the Hartree-Fock exchange potential. The two types of potentials U shown in Fig. 1 are simply different local approximations of the non-local kernel V-K.

c) Connection between GCM and RGM.

Although both methods, GCM and RGM, are equivalent in principle, it is difficult in practice to construct generating functions $\phi(\underset{\sim}{x},\underset{\sim}{r})$ such that, for given ϕ_A and ϕ_B, the model spaces spanned by (II.1) and (II.4) are identical. As an example where the equivalence of GCM and RGM can be shown

explicitly, let us assume that

$$\phi(\underset{\sim}{x},\underset{\sim}{r}) = \phi_{CM}\mathcal{A}\{\phi_A\phi_B\Gamma(\underset{\sim}{\rho},\underset{\sim}{r})\} \quad , \tag{II.10}$$

where Γ is a wave packet describing fluctuations of the relative motion coordinate $\underset{\sim}{\rho}$ around the mean distance $\underset{\sim}{r}$. Assumption (II.10) is fulfilled in the alpha-cluster model and the two-center harmonic oscillator shell model, provided the same oscillator length b is taken for both fragments. If $b_A \neq b_B$, or if more sophisticated models are used, the factorization property (II.10) breaks down, and a further integration is required to eliminate spurious center-of-mass excitations.

Combining eqs. (II.1) and (II.10) and comparing the result with eq. (II.4), one finds the desired connection between GCM and RGM as

$$g(\underset{\sim}{\rho}) = \int\Gamma(\underset{\sim}{\rho},\underset{\sim}{r})f(\underset{\sim}{r})d\underset{\sim}{r} \quad . \tag{II.11}$$

GCM matrix elements and RGM kernels are connected accordingly,

$$\int\Gamma(\underset{\sim}{\rho},\underset{\sim}{r})V(\underset{\sim}{\rho})\Gamma(\underset{\sim}{\rho},\underset{\sim}{r}')d\underset{\sim}{\rho} = \langle\phi(\underset{\sim}{r})|V_{AB}|\phi(\underset{\sim}{r}')\rangle_D \quad , \tag{II.12}$$

$$\int\Gamma(\underset{\sim}{\rho},\underset{\sim}{r})K(\underset{\sim}{\rho},\underset{\sim}{\rho}')\Gamma(\underset{\sim}{\rho}',\underset{\sim}{r}')d\underset{\sim}{\rho}d\underset{\sim}{\rho}' = \langle\phi(\underset{\sim}{r})|H_{eff}-E|\phi(\underset{\sim}{r}')\rangle - \langle\phi(\underset{\sim}{r})|H_{eff}-E|\phi(\underset{\sim}{r}')\rangle_D$$

where the subscript $_D$ indicates that antisymmetrization is only performed within the fragments A and B. By means of eqs. (II.12) it is possible to calculate the RGM kernels from the GCM matrix elements by defolding eqs. (II.12). This is important since direct calculation of the RGM kernels becomes impracticable with increasing particle number.

III. Effects of antisymmetrization.

a) Redundant states[10].

A peculiar feature of microscopic theories of composite particle scattering is the appearance of square-integrable states of relative motion which lead to solutions of eq. (II.7) at arbitrary energy. Such "redundant states" are obtained whenever the eigenvalue problem

$$(\text{III.1}) \qquad (\phi_A\phi_B|1 - \mathcal{A}|\phi_A\phi_B u) =: \int \mathcal{N}(\underset{\sim}{\rho},\underset{\sim}{\rho}')\, u(\underset{\sim}{\rho}')\, d\underset{\sim}{\rho}' = \lambda u(\underset{\sim}{\rho})$$

possesses solutions u^R with eigenvalue $\lambda=1$. After antisymmetrization, the corresponding many-body wave function

$$(\text{III.2}) \qquad \Psi^R = \mathcal{A}\{\phi_A\phi_B u^R\}$$

vanishes identically and provides a trivial solution of (II.5) at any energy E. Redundant states have to be counted in the Levinson theorem like true bound states,

$$(\text{III.3}) \qquad \delta_\ell(0) - \delta_\ell(\infty) = \pi(m_\ell + n_\ell) \quad ,$$

where m_ℓ is the number of redundant states in the ℓ^{th} partial wave, n_ℓ the number of true bound states. Redundant states actually occur if the internal states ϕ_A,ϕ_B are described in the oscillator shell model with equal b-values for both fragments, as has been used in most of the microscopic calculations done so far. In this model, the redundant states turn out to be harmonic oscillator wave functions with $N < N_R$ quanta excited, the redundancy limit N_R depending on the system under consideration.

The redundant states, which are a direct consequence of the Pauli principle, are important in two ways. First, eq. (III.3) shows that the Pauli principle can be simulated by extra bound states. This explains the "equivalence" of repulsive core and deep attractive potentials (Fig. 1). Second, the physical solutions g orthogonal to u^R are damped in the interaction region where absorption takes place. It is, therefore, not surprising that refractive and diffractive effects are often hard to disentangle (Fig. 2).

In more realistic models where the internal wave functions deviate from the pure oscillator shell model by the admixture of other configurations or by introducing different size parameters for different fragments, there will be eigenfunctions of $\mathcal{N}$ with eigenvalues λ close to 1. There have been controversial views regarding the nature of such "almost redundant states", - whether they are positive energy bound states[11] or resonances of finite width[12]. Careful studies on simple systems prove the latter version to be true.

Consider, e.g., the fictitious problem of dineutron-dineutron scattering[13] with the internal dineutron wave function taken as sum of two Gaussian functions with different widths $b \neq b'$. The nucleon-nucleon interaction is switched off artificially in order to study the effect of antisymmetrization separately. Fig.3 shows the phase $\delta_0(k)$, obtained by solving the resonating group equation (II.7). In the oscillator shell model limit, b=b', no resonance occurs, and the Levinson theorem is established as $\delta_0(0) - \delta_0(\infty) = \pi$ due to the presence of one redundant state.

Leaving the pure oscillator shell model by choosing $b \neq b'$ one observes a resonance whose width converges to a finite value if the step length d, used in the numerical treatment of eq. (II.7), is reduced. From the energy dependence one finds in this case $\delta_0(0) - \delta_0(\infty) = 0$ which demonstrates that no positive energy bound state is present. As a more realistic example, the α-^{16}O system has been studied[14] allowing for different size parameters, $b_\alpha \neq b_{^{16}O}$; again nuclear and Coulomb forces were turned off. The phases, shown in Figs. 4 and 5 for various partial waves ℓ, display the same general behaviour as in the dineutron case. For low ℓ-values the resonance structures are more complicated since several redundant states are degenerate.

On a formal basis [12,14] the finite width of the resonances and the discontinuous transition from "redundant" to "almost redundant" states can be explained as follows: Let us start from internal wave functions ϕ_A, ϕ_B in the harmonic oscillator model with $b_A = b_B + \eta$. The projector P onto the elastic channel can then be expanded in terms of the solutions u_i of eq. (III.1) as

$$P = \sum_i |\Psi_i\rangle\langle\Psi_i| \qquad \text{(III.4)}$$

where

$$\Psi_i = \left(\frac{n_A! n_B!}{(n_A+n_B)!}\right)^{\frac{1}{2}} (1-\lambda_i)^{-\frac{1}{2}} \mathcal{A}\{\phi_A \phi_B u_i\} \; ; \; \lambda_i \neq 1 \quad . \qquad \text{(III.5)}$$

Eq. (II.5) is then equivalent to

$$P\, H_{eff}\, P|\Psi\rangle = E\, P|\Psi\rangle \quad . \qquad \text{(III.6)}$$

To compare with the case $b_A = b_B$, we split P into

(III.7) $$P = P_o + P_1 \quad ,$$

such that P_o comprises those states u_i for which $\lambda_i \neq 1$ if $b_A \to b_B$. The resonating group equation (II.5) then reads

(III.8) $$P_o H_{eff} P_o |\Psi> = E\, P_o |\Psi>$$

for $b_A = b_B$. Eqs. (III.6) and (III.8) constitute two different problems because of the coupling term $P_o H_{eff} P_1$ appearing in (III.6). This term connects the P_o-space with states Ψ_i from P_1-space which describe internally excited fragments since

(III.9) $$(\phi_A \phi_B | \Psi_i) = \left(\frac{n_A! n_B!}{(n_A+n_B)!} \right)^{\frac{1}{2}} (1-\lambda_i)^{\frac{1}{2}} u_i(\underset{\sim}{\rho}) \to 0$$

for $\lambda_i \to 1$, and causes resonances in the spectrum of (III.6) which do not occur in (III.8).

Regarding the actual relevance of these resonances two points should be born in mind: i) The above results will be modified by the inclusion of Coulomb and nuclear forces. ii) The resonances appear at energies where inelastic channels ought to be included.

b) Alpha reduced widths.

Let Ψ_{A+4} denote the state vector of the (A+4)-system whose alpha-decay we wish to study. The probability for finding an alpha-particle at distance $\underset{\sim}{r}$ from the residual nucleus A is given by

(III.10) $$P(\underset{\sim}{r}) = |< \mathcal{A} \{ (1-\mathcal{N})^{-\frac{1}{2}} \delta(\underset{\sim}{\rho}-\underset{\sim}{r}) \phi_\alpha \phi_A \} | \Psi_{A+4} >|^2$$

where ϕ_α and ϕ_A are the internal wave functions of the

alpha-particle and the residual nucleus. The factor $(1-\mathcal{N})^{-\frac{1}{2}}$ is needed for normalization since

$$(III.11) \qquad \langle \mathcal{A}\{\delta(\underset{\sim}{\rho}-\underset{\sim}{r})\phi_\alpha\phi_A\}\,|\,\mathcal{A}\{\delta(\underset{\sim}{\rho}-\underset{\sim}{r}')\phi_\alpha\phi_A\}\rangle = \delta(\underset{\sim}{r}-\underset{\sim}{r}') - \mathcal{N}(\underset{\sim}{r},\underset{\sim}{r}')$$

contains the orthonormality defect $\mathcal{N}(\underset{\sim}{r},\underset{\sim}{r}')$ due to antisymmetrization between the fragments.

For the interpretation of $P(\underset{\sim}{r})$ as probability it is crucial to include the factor $(1-\mathcal{N})^{-\frac{1}{2}}$ in eq. (III.10). Then

$$(III.11) \qquad \Pi(\underset{\sim}{r}) = |\mathcal{A}\{(1-\mathcal{N})^{-\frac{1}{2}}\delta(\underset{\sim}{r}-\underset{\sim}{\rho})\phi_\alpha\phi_A\}\rangle\langle\{\phi_A\phi_\alpha\delta(\underset{\sim}{r}-\underset{\sim}{\rho})(1-\mathcal{N})^{-\frac{1}{2}}\}\mathcal{A}|$$

is a projector, and

$$(III.12) \qquad P(\underset{\sim}{r}) = \langle\Psi_{A+4}|\Pi(\underset{\sim}{r})|\Psi_{A+4}\rangle$$

is a probability if Ψ_{A+4} is normalized.

The actual importance of the factor $(1-\mathcal{N})^{-\frac{1}{2}}$ (discarded in the traditional approach) has been demonstrated recently by Fliessbach[5]. It accounts for a factor 10 - 1000, depending on the system under consideration, and leads to reduced widths in excellent agreement with experiment. It is proper treatment of antisymmetrization which is responsible for this effect! One expects similar effects for spectroscopic factors of alpha- and two-particle-transfer. There is no normalization problem for spectroscopic factors in the case of one-particle-transfer where the operator $\mathcal{N}$ has only eigenvalues 0 and 1. One simply has to discard the redundant states (eigenvalue 1), - the remainder of $(1-\mathcal{N})$ then reduces to the unit operator.

IV. Absorption.

Most of the microscopic calculations done so far neglect absorption completely. They use real effective interactions (like, e.g., the Volkov force), adapted to the system at infinite fragment separation, and are at best useful approximations at low energies. Simple approaches[15] which introduce absorption phenomenologically in the Hill-Wheeler or resonating group eqs., (II.2) and (II.7), cannot solve the problem of energy dependence and radial shape of the optical potential. The first genuine microscopic approach is due to Toepffer et al.[16]

Their work is based on the G-matrix concept of Brückner. For simplicity they treat fragments A and B as two Fermi spheres approaching each other with relative initial momentum K. At given mean distance $\underset{\sim}{r}$ between A and B, the system is described by a Slater determinant $\phi(\underset{\sim}{r},\underset{\sim}{K})$ built from single-particle states

$$|\underset{\sim}{k};\underset{\sim}{r}_A,\underset{\sim}{K}_A\rangle \hat{=} \exp\{i(\underset{\sim}{k}+\underset{\sim}{K}_A)\cdot(\underset{\sim}{x}-\underset{\sim}{r}_A)\} \tag{IV.1}$$

for, e.g., a nucleon in fragment A. Here

$$\underset{\sim}{r} = \underset{\sim}{r}_A - \underset{\sim}{r}_B \quad ; \quad \underset{\sim}{K} = \tfrac{1}{2}(\underset{\sim}{K}_A - \underset{\sim}{K}_B) \quad . \tag{IV.2}$$

The energy expectation value $E(\underset{\sim}{r},\underset{\sim}{K})$ for A and B being separated by $\underset{\sim}{r}$ and $\underset{\sim}{K}$ in ordinary space and momentum space, resp., is calculated as:

$$E(\underset{\sim}{r},\underset{\sim}{K}) = \langle\phi(\underset{\sim}{r},\underset{\sim}{K})|T + G|\phi(\underset{\sim}{r},\underset{\sim}{K})\rangle \tag{IV.3}$$

where T is the kinetic energy and G the two-body G-matrix,

$$G = V + V \frac{Q_o}{(\omega - T + i\eta)} G \quad . \tag{IV.4}$$

The Pauli operator Q_o excludes single-particle states occupied in $\phi(\underset{\sim}{r},\underset{\sim}{K})$ as intermediate states, hence $G = G(\underset{\sim}{r},\underset{\sim}{K})$. V is a realistic nucleon-nucleon interaction and ω the starting energy. The optical potential $U(\underset{\sim}{r},\underset{\sim}{K})$ is then identified with the interaction energy

$$\frac{1}{2} \sum_{\substack{m \neq A \\ n \neq B}} \langle mn; \underset{\sim}{r},\underset{\sim}{K} | G(\underset{\sim}{r},\underset{\sim}{K}) | mn; \underset{\sim}{r},\underset{\sim}{K} \rangle = U(\underset{\sim}{r},\underset{\sim}{K}) \tag{IV.5}$$

contained in (IV.3). In contrast to ordinary Brückner theory, $U(\underset{\sim}{r},\underset{\sim}{K})$ is complex for $K > 0$. Apart from virtual excitations, responsible for the dispersive part of G, there can be real excitations when kinetic energy of relative motion is converted into internal excitation energy, giving rise to an absorptive part,

$$G = V + V\mathcal{P}\left(\frac{Q_o}{\omega - T}\right) G - i\pi V Q_o \delta(\omega - T) G \quad . \tag{IV.6}$$

There are a number of shortcomings of the method of Toepffer et al. in its present form:

i) Surface and shell effects are neglected when using the plane wave basis (IV.1). To improve on this point we switch to a basis of moving oscillator functions

$$|\underset{\sim}{k}; \underset{\sim}{r}_A, \underset{\sim}{K}_A\rangle \rightarrow |\alpha; \underset{\sim}{r}_A, \underset{\sim}{K}_A\rangle \tag{IV.7}$$

where

$$|\alpha; \underset{\sim}{r}_A, \underset{\sim}{K}_A\rangle \hat{=} \exp\{i\underset{\sim}{K}_A \cdot (\underset{\sim}{x} - \underset{\sim}{r}_A) - (\underset{\sim}{x} - \underset{\sim}{r}_A)^2\} H_\alpha(\underset{\sim}{x} - \underset{\sim}{r}_A) \tag{IV.8}$$

for particles belonging to fragment A. Technically this step amounts to calculating the expansion coefficients $\langle\alpha\beta;\underset{\sim}{r},\underset{\sim}{K}|\underset{\sim}{k},\underset{\sim}{k}';\underset{\sim}{r},\underset{\sim}{K}\rangle$ of two-particle states by Fourier transformation.

ii) Toepffer et al. approximate the operator Q_o in the model of overlapping Fermi spheres such that the exclusion principle is fulfilled on average only. In the moving oscillator basis the Pauli operator Q_o reads

$$Q_o = 1 - \sum_{\substack{\alpha\beta\gamma\delta \\ \text{occupied}}} B^{-1}_{\alpha\gamma}|\alpha\beta;\underset{\sim}{r},\underset{\sim}{K}\rangle\langle\gamma\delta;\underset{\sim}{r},\underset{\sim}{K}|B^{-1}_{\beta\delta} \tag{IV.9}$$

where B is the overlap matrix in the non-orthogonal basis of moving oscillator states (IV.8). As expected Q_o tends to 1 for high energies since

$$\cdot\ \langle\underset{\sim}{k}_1,\underset{\sim}{k}_2;\underset{\sim}{r},\underset{\sim}{K}|Q_o|\underset{\sim}{k}_1,\underset{\sim}{k}_2;\underset{\sim}{r},\underset{\sim}{K}\rangle\ -1 \propto \exp\{-K^2\}\ , \tag{IV.10}$$

the influence of the Pauli principle on absorption disappears with increasing energy.

iii) The simplest way to connect the G-matrix (IV.4) with two-nucleon scattering data is to iterate eq. (IV.4) and replace V by the two-nucleon $\mathcal{T}$-matrix,

$$G \approx V + V\,\frac{Q_o}{\omega - T + i\eta}\,\mathcal{T} + \ldots . \tag{IV.11}$$

To improve the convergence of this expansion we introduce a reference matrix

$$\tilde{G} = G(r \to \infty, K \to 0) \tag{IV.12}$$

which is related to G through

$$G = \bar{G} + \bar{G}\left(\frac{Q_o}{\omega - T + i\eta} - \frac{\bar{Q}_o}{\omega - \bar{T}}\right)G \quad . \tag{IV.13}$$

The Pauli operator $\tilde{Q}_o$ of the reference problem as well as G are real as they refer to a bound state problem (separated fragments at rest). One expects that the iteration of (IV.13) converges faster than for (IV.4). We obtain to second order:

$$\mathrm{Re}\ G = \tilde{G} + \tilde{G}\mathcal{P}\left(\frac{Q_o - \bar{Q}_o}{\omega - T}\right)\tilde{G} \tag{IV.14}$$

and

$$\mathrm{Im}\ G = -\pi \tilde{G} Q_o \delta(\omega - T)\tilde{G} \quad . \tag{IV.15}$$

As reference matrix we may take a Volkov or Skyrme force.

iv) Relative motion is treated incorrectly when interpreting (IV.5) as optical potential since the parameter $\underset{\sim}{r}$ differs from the dynamical variable of relative motion $\underset{\sim}{\rho}$. In other words, eq. (IV.5) neglects non-diagonal elements $\langle \phi(\underset{\sim}{r}', \underset{\sim}{K}) | G | \phi(\underset{\sim}{r}, \underset{\sim}{K}) \rangle$. They can be taken care of by using the above matrix elements as input for the Hill-Wheeler eqs. (II.2) in the symmetrized form:

$$\frac{1}{2}\langle \phi(\underset{\sim}{r}', \underset{\sim}{K}) | G(\underset{\sim}{r}', \underset{\sim}{K}) + G(\underset{\sim}{r}, \underset{\sim}{K}) | \phi(\underset{\sim}{r}, \underset{\sim}{K}) \rangle \quad . \tag{IV.16}$$

This procedure is not fully self-consistent since the above G is calculated with respect to a single configuration $\phi(\underset{\sim}{r}, \underset{\sim}{K})$ of the two-center shell model, which covers only part of the GCM-space of functions defined by (II.1).

It remains to investigate whether it is justified to use the G-matrix of eq. (IV.4) as effective force in the elastic channel. Following Feshbach[8] the effective Hamiltonian can be expressed as

$$H_{eff} = P\{H + HQ(E-QHQ+i\eta)^{-1}QH\}P \tag{IV.17}$$

where P projects onto the elastic channel defined in (II.1) and

$$Q = 1 - P \tag{IV.17'}$$

Let us split H into

$$H = H_o + V \tag{IV.18}$$

such that

$$QH_o = H_oQ \quad ; \tag{IV.19}$$

then eq. (IV.17) can be rewritten as

$$H_{eff} = P\{H_o + \mathcal{G}\}P \tag{IV.20}$$

where

$$\mathcal{G} = V + V\frac{Q}{E-H_o+i\eta}\mathcal{G} \tag{IV.21}$$

is in general a many-body operator. In the independent pair approximation $\mathcal{G}$ reduces to the two-body operator G of eq. (IV.4) if we choose $H_o=T$.

Within their G-matrix concept Toepffer et al.[16] have studied elastic ^{16}O-^{16}O scattering. The imaginary part of the optical potential (IV.5) is shown in Fig. 6 for various energies. It shows surface transparency and the energy dependence is almost linear upto 80 MeV c.m. energy. The latter point will be modified when shell effects are included as described in IV.i). Surface transparency may become more pronounced if the GCM

diagonal elements are replaced by the proper resonating group kernels. The excitation function (Fig. 7) at $\theta_{c.m.} = 90^0$ is in satisfactory agreement with experiment, in particular at high energies. At low energies the calculation shows too little structure which is probably due to the poor treatment of the real part of the optical potential, chosen as phenomenological local potential of Woods-Saxon type. This can be improved by proper calculation of the real part within the RGM where resonance structures are found (Fig. 8) at low energies[17]. They will be modified regarding width and position when absorption is included.

V. Conclusion.

A method has been presented by which Pauli principle and absorption can be treated consistently on a microscopic level.[18] Once the internal fragment wave functions and the effective nucleon-nucleon force at infinite fragment separation are chosen, there is no free parameter in the theory. The method is rather flexible since the intermediate states in the G-matrix equation depend on the separation $\underset{\sim}{r}$ and include two particle-two hole excitations in the compound system as well as particle-hole excitations of the individual fragments. In view of the substantial numerical work involved, the method will not be suitable for large scale calculations throughout the periodic table but only for a few simple

representative systems. This should suffice to learn about proper parametrization of optical potentials to be used for analyzing experimental data.

Acknowledgements.

The author wishes to thank the Council for Scientific and Industrial Research for support during his stay at the Nuclear Physics Research Unit, Witwatersrand University, Johannesburg, where this work was initiated. It is also sponsored by the Bundesministerium für Forschung und Technologie.

References

1.) D.M. Brink and F. Stancu, Nucl.Phys. A243 (1975) 175

2.) H. Löhner, H. Eickhoff, D. Frekers, S. Gaul, K. Poppensieker, R. Santo, A.G. Drentje and L.W. Put, preprint Universität Münster and Rijksuniversiteit Groningen (1977).

3.) W. Frahn in: Heavy Ion, High-Spin States and Nuclear Structure, Vol. I, I.A.E.A. (Vienna 1975).

4.) D.H. Gross, see ref. 3.)

5.) T. Fliessbach, Z.Physik A272 (1975) 39; Z.Physik A277 (1976) 151.

6.) Generator coordinate method for nuclear bound states and reactions, Fizika 5 (1973) Suppl., ed. by M.V. Mihailović and M. Rosina; C.W. Wong, Physics Reports 15C (1974) 283.

7.) K. Wildermuth and W. McClure, Springer Tracts in Modern Physics 41 (Springer, Berlin, 1966).

8.) H. Feshbach, Ann. of Physics 5 (1958) 357; 19 (1962) 287.

9.) The Resonating Group, Phys.Letters 43B (1973) 165; H. Friedrich, H. Hüsken and A. Weiguny, Nucl.Phys. A 220 (1974) 125; R. Beck, J. Borysowicz, D.M. Brink and M.V. Mihailović, Nucl.Phys. A 244 (1975) 45, 58.

10.) H. Feshbach, Ann. of Physics 19 (1962) 287.

11.) D. Clement, E.W. Schmid and A.G. Teufel, Phys. Letters 49B (1974) 308.

12.) S. Saito, S. Okai and R. Tamagaki, Progr.Theoret.Phys. 50 (1973) 1561.

13.) A. Böinghoff, H. Hüsken and A. Weiguny, Phys.Letters 61B (1976) 9.

14.) A. Böinghoff, diploma thesis, Universität Münster (1977).

15.) W. Sünkel and K. Wildermuth, Phys.Letters 41B (1972) 439; L.F. Canto, Nucl.Phys. A279 (1977) 97; D. Frekers and K. Langanke, preprint, Universität Münster (1977).

16.) D.A. Saloner and C. Toepffer, Nucl.Phys. A283 (1977) 108; D.A. Saloner, C. Toepffer and B. Fink, Nucl.Phys. A283 (1977) 131.

17.) H. Friedrich, Nucl.Phys. A224 (1974) 537.

18.) C. Toepffer, W. Gadinabokao and A. Weiguny, in preparation.

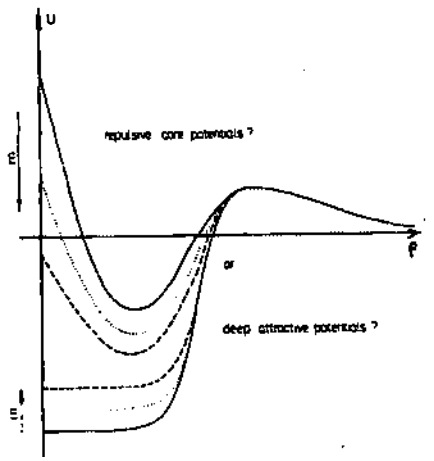

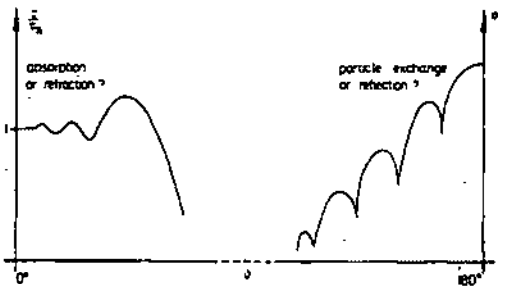

Fig. 1. Qualitative behaviour of some heavy ion potentials for various energies.

Fig. 2. Qualitative features of the elastic scattering cross section.

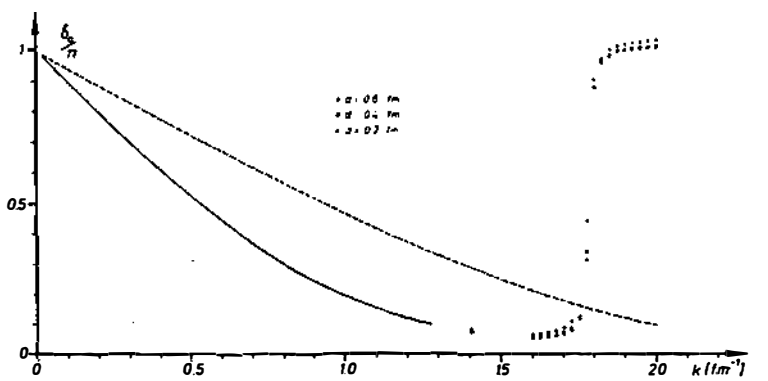

Fig. 3. S-wave phase shift caused by the Pauli principle in dineutron-dineutron scattering, taken from ref.13.). The dashed curve refers to b = b' = 1 fm and the solid line to b = 2b' = 2 fm; near resonance the phase is displayed for various step lengths d.

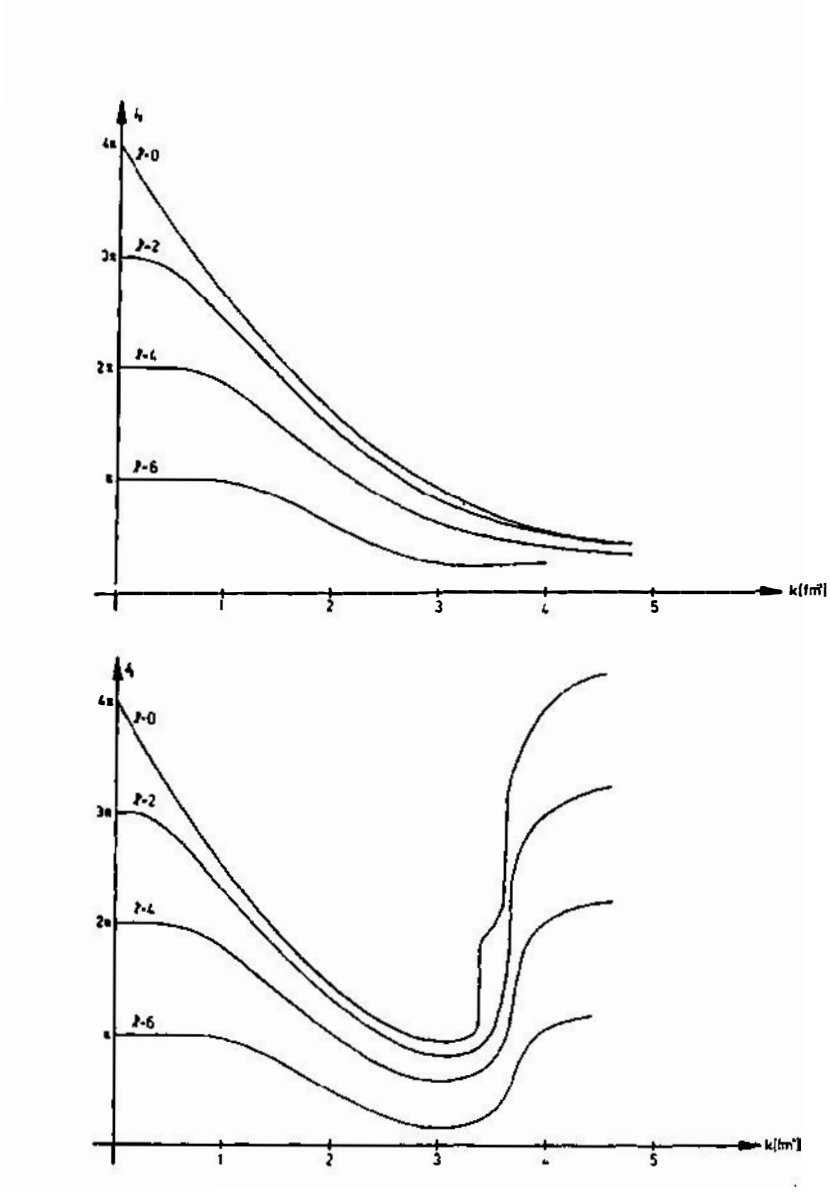

Fig. 4. α-^{16}O phase shifts for even partial waves, taken from ref. 14.). The upper part refers to $b_\alpha = b_{^{16}O}$, the lower one to $b_\alpha \neq b_{^{16}O}$.

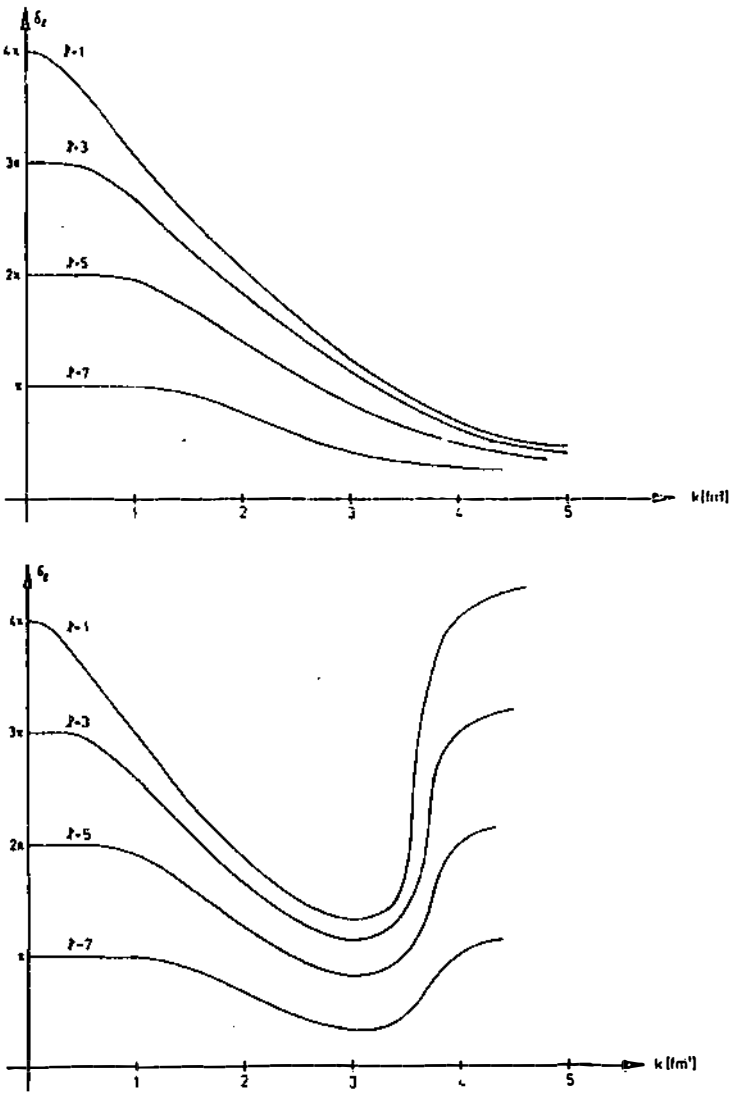

Fig. 5. α-^{16}O phase shifts for odd partial waves, taken from ref. 14.). The upper part refers to $b_\alpha = b_{^{16}O}$, the lower one to $b_\alpha \neq b_{^{16}O}$.

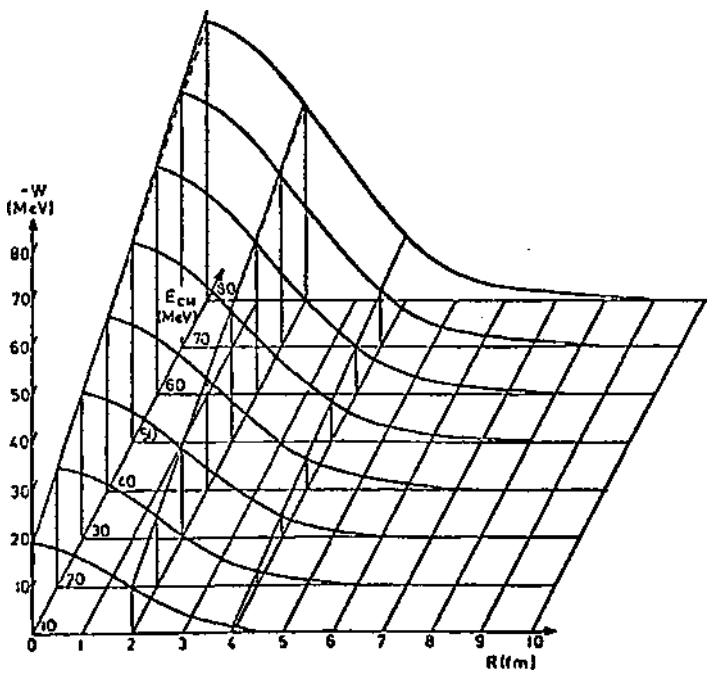

Fig. 6. Imaginary part of the ^{16}O-^{16}O optical potential as function of the separation distance at various c.m. energies (ref.16).

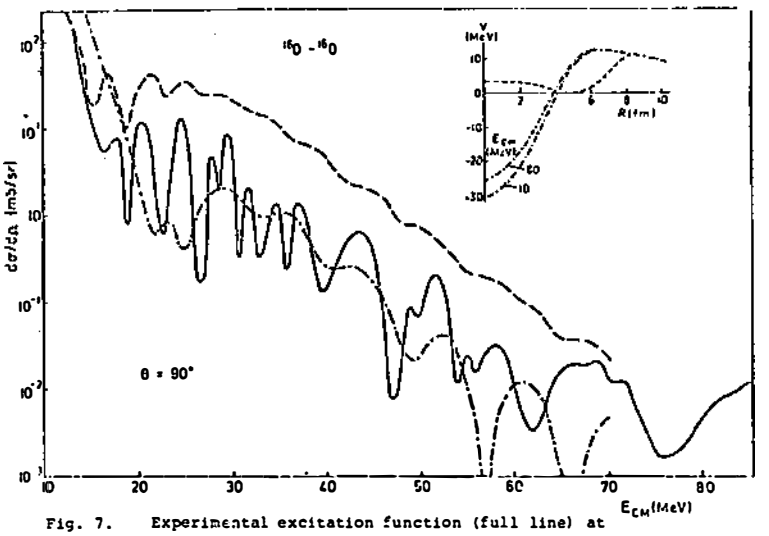

Fig. 7. Experimental excitation function (full line) at $\vartheta_{c.m.} = 90°$ for elastic ^{16}O-^{16}O scattering. Dashed and dashed-dotted lines are obtained with the G-matrix approach by Toepffer et al. (ref. 16) for the imaginary part of the optical potential; the real part is shown in the insert.

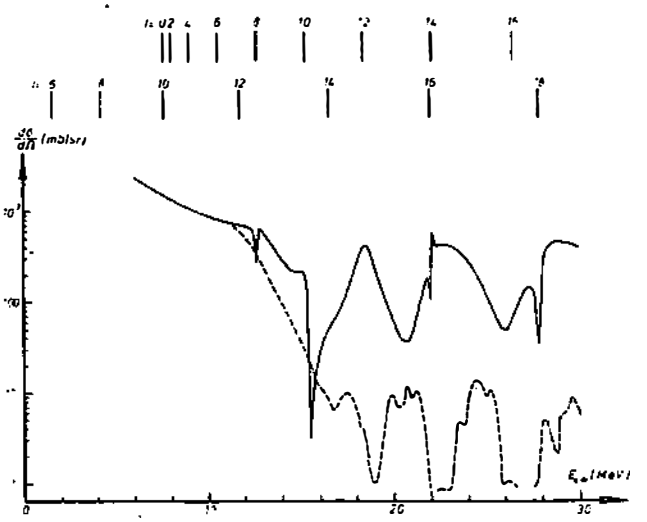

Fig. 8. ^{16}O-^{16}O elastic scattering cross section at $\vartheta_{c.m.} = 90°$. The theoretical curve (full line) stems from a resonating group calculation by Friedrich (ref. 17) where absorption is neglected completely.

DISCUSSION

A. Tohsaki-Suzuki: How do you connect the RGM and the GCM kernels for the case of scattering of nuclei described by different oscillator parameters? I think the effect coming from the c.m. motion plays a minor role in the scattering problem without compound process. Do you think so?

A. Weiguny: If you work within the GCM a further (3-dimensional) integration is required to remove spurious center-of-mass effects when using different oscillator lengths. A method to calculate RGM kernels from GCM matrix elements for fragments with different oscillator lengths has been proposed by Giraud and Letourneux.

H. Shimoda: Having microscopic results of W could you tell us which phenomenological absorption potentials fit into this picture.

A. Weiguny: From the results of Toepffer et al. we learn that absorption does not take place on the surface. One has volume absorption with some surface transparency.

Y.C. Tang: Through the generalized Levinson theorem, you seem to suggest that the effective internuclear potential is a deep potential well. Do you have any suggestion to justify the use of a repulsive-core potential to represent the effective interaction between two nuclei?

A. Weiguny: There are many phase-equivalent local approximations to the correct non-local effective internuclear potential. The deep attractive potential is one possibility where the effect of the Pauli principle is simulated with the help of the generalized Levinson theorem. The repulsive core potential is the simplest way to account for the repulsive nature of the Pauli principle.

K. Goeke: **There exists a rather old problem in applying the GCM, and probably the RGM: In the case of uniform translations it is known that the GCM gives a mass, which is not identical to the total mass of the moving system, as it should be due**

to Galileian invariance. This gave rise to the introduction of a conjugate generator momentum (the double projection formalism of Peierls and Thouless). Of course, one can make the particular case of translations right, but nevertheless this raises doubts whether GCM is, strictly speaking, correct if one uses it in the usual way. Another example: the mass of adiabatic time dependent Hartree-Fock and GCM are different. However, if one uses also the integration over the conjugate momentum in GCM, then they are identical.

A. Weiguny: The problem concerning the total mass for translational motion appears when the generating functions violate Galileian invariance. There is no such invariance principle for rotations and vibrations. In general, the choice of the generating functions requires some intuition. If you don't trust your intuition, you can test the initial choice of generating functions by admixing other configurations, as mentioned in Prof. Tang's talk. I agree with you that, when transforming the GCM integral equation into some differential equation of Schrödinger type, one should use both position and momentum like parameters. This is connected with well-known mathematical peculiarities of the GCM.